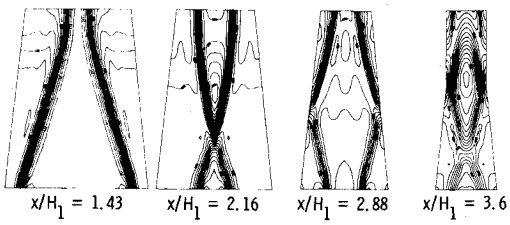

Fig. 3 Pressure contours at various axial locations ($M_1 = 5.0$, $\Lambda = 45$ deg).

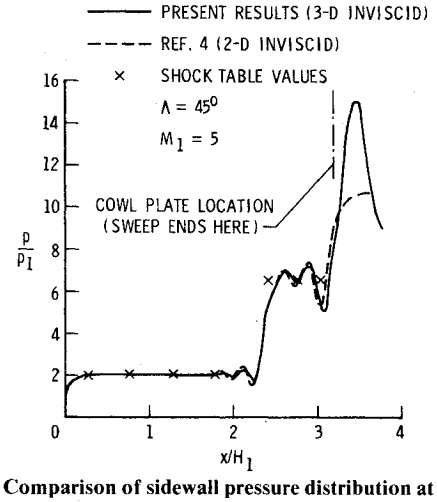

Fig. 4 Comparison of sidewall pressure distribution at $z/H_1 = 0$.

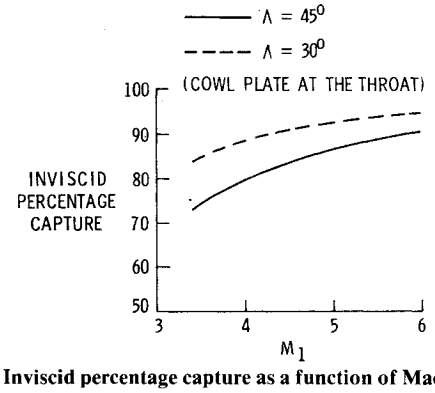

Fig. 5 Inviscid percentage capture as a function of Mach number.

plots clearly show the shock and expansion waves and their interactions with each other and with boundaries.

Figure 4 shows the sidewall pressure distribution at $M_1 = 5.0$. The present results are compared with the pressure distribution obtained from the shock tables and with the two-dimensional analysis of Ref. 4. It is seen that the present distribution is in very good agreement with the other results up to the point of cowl closure. Beyond this point, the present analysis predicts much higher pressure due to the cowl shock which cannot be accounted for in two-dimensional analysis.

As mentioned earlier, the purpose of the sidewall sweep is to turn the flow downward, which results in some flow spilling out of the inlet ahead of the cowl plate. This provides the potential to operate over a range of Mach numbers even with a fixed-geometry inlet. The quantity of the flow captured by the inlet is a very important quantity in its performance calculations and needs to be estimated. Figure 5 shows the inviscid flow captured by the inlet as a function of Mach number for two sidewall sweep angles. These capture calculations are made with the cowl located at the minimum area section. The flow captured by the inlet with 45-deg sweep varies from 91% at $M_1 = 6.0$ to 72.5% at $M_1 = 3.4$. The capture with the 30-deg sweep is higher and varies from 94.5% at $M_1 = 6.0$ to 84% and $M_1 = 3.4$. In the calculations of the flow capture, the spillage due to the pressure differential between the inside and outside of the inlet has not been included. Of course, the viscous effects, which are not considered here, will also result in some decrease in the flow capture.

The preceding results are typical of the quantitative calculations that can be made with the present analysis. The numerical code can be very helpful in screening the inlet configurations by making similar calculations for other parametric variations of the basic geometry.

References

[1] Jones, R.A. and Huber, P.W., "Toward Scramjet Aircraft," *Astronautics & Aeronautics*, Vol. 16, Feb. 1978, pp. 38-49.

[2] Beach, H.L. Jr., "Hypersonic Propulsion," Paper XII, NASA CP-2092, May 1979.

[3] Trexler, C.A., "Design and Performance at a Local Mach Number of 6 of an Inlet for an Integrated Scramjet Concept," NASA TN D-7944, 1975.

[4] Kumar, A., "Numerical Analysis of the Scramjet Inlet Flow Field Using Two-Dimensional Navier-Stokes Equations," NASA TP-1940, Dec. 1981.

[5] Smith, R.E. and Weigel, B.L., "Analytic and Approximate Boundary-Fitted Coordinate Systems for Fluid Flow Simulation," AIAA Paper 80-0192, 1980.

[6] MacCormack, R.W., "The Effect of Viscosity in Hypervelocity Impact Cratering," AIAA Paper 69-354, 1969.

[7] Kumar, A., "Three-Dimensional Inviscid Analysis of the Scramjet Inlet Flow Field," AIAA Paper 82-0060, 1982.

AIAA 82-4243

Higher-Order Flow Angle Corrections for Three-Dimensional Wind Tunnel Wall Interference

Magdi H. Rizk*
Flow Research Company, Kent, Washington

Nomenclature

c = chord
C_L = lift coefficient
l = semispan
L = spanwise lift distribution
M = Mach number
S = lifting surface
x = coordinate in the undisturbed flow direction
x_0 = $0.5\,(x_L + x_T)$
x_L = x coordinate of leading edge
x_T = x coordinate of trailing edge
y = coordinate normal to model plane of symmetry
z = vertical coordinate in the upward direction
Z = vertical coordinate of mean lifting surface
α = angle of attack
γ = lift distribution
τ = maximum height of parabolic arc

Superscripts and Subscripts

c = correction
ce = exact correction
F = free air corrected condition

Received March 15, 1982.

*Senior Research Scientist. Member AIAA.

FP = flat plate
PA = parabolic arc
sc = section correction
T = tunnel condition
t = tail
w = wing
I = corrected angle of attack derived by using Eq. (2) for α^{sc}
II = corrected angle of attack derived by using Eq. (8) for α^{sc}
∞ = undisturbed conditions

Introduction

MOKRY and Ohman[1] used the classical approach in finding Mach number and angle-of-attack corrections for two-dimensional problems, but they used measured pressure distributions in lieu of the less accurate, homogeneous wall boundary conditions. (Classical methods for predicting wind tunnel wall interference corrections have been summarized by Garner et al.[2]) They calculated the interference flow numerically using the fast Fourier transform technique.

The recent work of Rizk and Smithmeyer[3] extends the two-dimensional method of Mokry and Ohman to three-dimensional flows about aircraft configurations and eliminates the requirement that the model be much smaller than the tunnel size. The correction flow (which is the negative of the wall interference flow) is assumed to satisfy the Prandtl-Glauert equation, subject to boundary conditions near the tunnel walls. Since the correction flow is the difference between the free-air flow and the tunnel flow, this difference needs to be known at the boundaries to apply the correct conditions there. At the boundaries, the tunnel flow is determined from wind tunnel measurements while the free-air flow is obtained from a truncated series describing the free-air solution. The correction flow contains the necessary information to determine the wing and tail angle-of-attack corrections and the Mach number correction. In determining the angle-of-attack corrections, this method neglects camber corrections, leading to inaccuracies in the predicted corrections. In the present work, higher order angle-of-attack corrections which correspond to camber corrections are included, leading to improved results.

Formulation

A lifting surface, S^T, tested in a wind tunnel at an angle of attack $\alpha=\alpha^T$ and an undisturbed Mach number $M_\infty=M_\infty^T$ develops a lift distribution $\gamma(x,y)$. The lifting surface S^F which develops the same lift distribution $\gamma(x,y)$ when tested in free air with $M_\infty=M_\infty^T$ is the corrected lifting surface. The correction Z^c to the mean lifting surface is given by

$$Z^c(x,y)=Z^F(x,y)-Z^T(x,y)$$

Since it is desirable to have similar geometrical configurations for the wind tunnel and free-air models, wall interference correction procedures seek to find the corrected angle of attack α^F which nearly produces the lift distribution $\gamma(x,y)$ for S^T in free air. In Ref. 3 the angle-of-attack correction is evaluated using the formula

$$\alpha^c=\frac{\int_{-l}^{l}\alpha^{sc}(y)\,|L^T(y)|\,dy}{\int_{-l}^{l}|L^T(y)|\,dy} \tag{1}$$

and the angle-of-attack correction at a given spanwise station $\alpha^{sc}(y)$ is calculated from the relation

$$\alpha^{sc}(y)=-[1/c(y)]\int_{x_L(y)}^{x_T(y)}Z_x^c(x,y)\,dx \tag{2}$$

In this Note, a more accurate evaluation for $\alpha^{sc}(y)$ is derived, improving the accuracy of the predicted angle-of-attack correction.

The slope of the mean lifting surface correction is expanded in a Taylor series as follows:

$$Z_x^c(x,y)=Z_x^c[x_0(y),y]+[x-x_0(y)]\,Z_{xx}^c[x_0(y),y] \tag{3}$$

where higher-order terms have been neglected. The first term in the expansion indicates that the lowest-order correction is an angle-of-attack correction. The second term corrects the camber shape by adding a parabolic arc correction to the original shape. Higher-order camber corrections have been neglected here. Substituting the expansion for Z_x^c into Eq. (2), it is found that

$$\alpha^{sc}(y)=-Z_x^c[x_0(y),y] \tag{4}$$

Therefore the correction used in Ref. 3 is a first-order correction, which differs from the present lowest-order correction by higher-order terms not considered here.

Including the second-order term as it appears in Eq. (3) will produce a change in the shape of the lifting surface. This can be avoided by finding an angle-of-attack correction which produces the same lift correction introduced by the parabolic arc. In an incompressible flow, the lift coefficient for a flat plate at an angle of attack α is given by

$$C_L^{FP}=2\pi\alpha \tag{5}$$

while the lift coefficient of the parabolic arc which is defined by

$$z=z^{PA}=4\tau\left[\frac{1}{4}-\frac{(x-x_0)^2}{c^2}\right] \qquad -\frac{c}{2}<x-x_0<\frac{c}{2} \tag{6}$$

is given by[4]

$$C_L^{PA}=4\pi\tau/c \tag{7}$$

From the above expressions it can be concluded that a flat plate of length c at an angle of attack α will have the same lift as the parabolic arc described by Eq. (6) if

$$\alpha=2\tau/c=-(c/4)z_{xx}^{PA}$$

This is true for compressible linearized flows as well as incompressible flows. The expression for α^{sc}, which includes both angle-of-attack and camber effects, can then be written as

$$\alpha^{sc}(y)=-\{Z_x^c[x_0(y),y]+(c/4)Z_{xx}^c[x_0(y),y]\} \tag{8}$$

The corrected angle of attack, α^F, is given by

$$\alpha^F=\alpha^T+\alpha^c$$

Results and Discussion

Angle-of-attack corrections are calculated for the wing-tail configuration in a solid-wall wind tunnel as shown in Fig. 1. The dashed lines in the figure indicate the boundaries of the boundary value problem for the correction flow. The wing angle of attack is chosen to be 3 deg, while the tail angle of attack is chosen to be 4 deg. The undisturbed wind tunnel Mach number M_∞^T is taken to be 0.7, and a NACA 0012 airfoil section is used for both the wing and the tail.

Table 1 compares the angle-of-attack corrections obtained with the absence of the tail by the first-order theory using Eq. (2), the first-order theory using Eq. (4), the second-order theory using Eq. (8), and the correction α^{ce}, which is the value of α^c required for the wind tunnel and free-air lift values to

Table 1 Angle-of-attack corrections

	First-order theory, Eq. (2)	First-order theory, Eq. (4)	Second-order theory, Eq. (8)	Exact theory
α^c, deg	0.53	0.56	0.75	0.90
$(\alpha^c - \alpha^{ce})/\alpha^{ce}$	−0.41	−0.38	−0.17	0

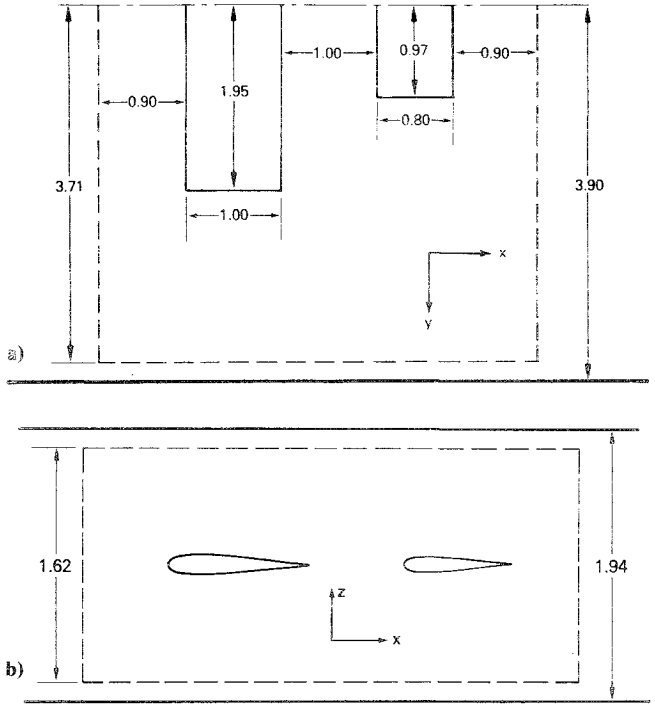

Fig. 1 Wing-tail in tunnel: a) top view, b) side view.

match exactly.[5] Note that the solution of Ref. 5 is obtained by a line relaxation scheme which is less efficient than the fast solver used to obtain the current solution.

A comparison between the spanwise lift distribution for the wind tunnel flow ($\alpha_w = 3$ deg, $\alpha_t = 4$ deg), the free-air flow at the corrected conditions derived from first-order theory of Eq. (2) ($\alpha_w = 3.52$ deg, $\alpha_t = 5.32$ deg), the free-air flow at the corrected conditions derived from second-order theory ($\alpha_w = 3.74$ deg, $\alpha_t = 5.37$ deg), and the free-air flow at the uncorrected conditions ($\alpha_w = 3$ deg, $\alpha_t = 4$ deg) is given in Fig. 2. In order to compare the accuracy of the different theories, Mach number corrections have not been included. The undisturbed Mach number has been held fixed at the tunnel value of 0.7 for all cases.

Table 1 as well as Fig. 2 indicate improved accuracy for the second-order theory over the first-order theory. The discrepancy in the lift distributions between the second-order theory and the tunnel flow shown in Fig. 2 is due to neglecting higher-order terms in Eq. (3), making some two-dimensional assumptions in applying Eqs. (1), (5), and (7), and using a truncated series to derive the free-air boundary conditions.[3]

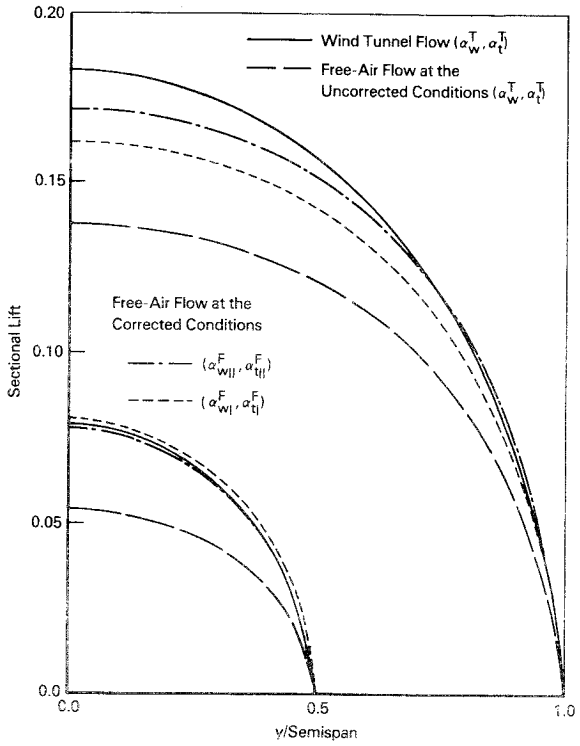

Fig. 2 Spanwise lift distribution for wing and tail.

Concluding Remarks

A second-order theory which includes camber effects in wind tunnel wall interference corrections has been developed. The camber correction is introduced as an equivalent angle-of-attack correction, thereby avoiding changes in the geometrical configuration of the tested model. Examples presented indicate improved results for the second-order theory over the first-order theory, which neglects camber effects.

Acknowledgment

This work was sponsored by NASA Langley under Contract NAS1-16262.

References

[1] Mokry, M. and Ohman, L.H., "Application of the Fast Fourier Transform to Two-Dimensional Wind Tunnel Wall Interference," *Journal of Aircraft*, Vol. 17, June 1980, pp. 402-408.

[2] Garner, H.C. et al., "Subsonic Wind Tunnel Wall Corrections," AGARDograph 109, Oct. 1966.

[3] Rizk, M.H. and Smithmeyer, M.G., "Wind Tunnel Wall Interference Corrections for Three-Dimensional Flows," *Journal of Aircraft*, Vol. 19, June 1982, pp. 465-472.

[4] Von Mises, R., *Theory of Flight*, Dover Publications, Inc., New York, 1959, pp. 198-208.

[5] Rizk, M.H., "A New Optimization Technique Applied to Wind Tunnel Angle-of-Attack Corrections," Flow Research Company, Kent, Wash., Note No. 198, Feb. 1982.